***inter.noise 2000***
***The 29th International Congress and Exhibition on Noise Control Engineering***
***27-30 August 2000, Nice, FRANCE***

**I-INCE Classification:** 7.2

# NEARFIELD HOLOGRAPHY FOR ARBITRARILY SHAPED STRUCTURES

**J. Maynard**

Penn State University, 104 Davey Laboratory, 16802, University Park, PA, United States Of America

Tel.: 814 865-6353 / Fax: 814 865-3604 / Email: maynard@phys.psu.edu

**Keywords:**
NEARFIELD, SPHERICAL, HOLOGRAPHY, WAVEFUNCTION

**ABSTRACT**
Nearfield acoustic holography has been shown to be a powerful tool for the study of sound radiation from vibrating structures. In the most manageable form of holography, reconstructions of the surface of the source can be obtained if the surface coincides with a level surface of a separable coordinate system. At Penn State University a new technique using spherical wavefunctions and singular value decomposition was developed for holographically reconstructing arbitrarily shaped sources. Computer implementations have become feasible with the availability of high speed computers. A successful application of the technique was an explanation of the measured radiation damping of elastic solids in a high density gas.

## 1 - INTRODUCTION

An important operation in Nearfield Acoustic Holography (NAH), and in many theoretical and measurement techniques in noise control, is the calculation of the sound field radiated by a source with a known surface velocity. Two common methods for performing calculations are a) using a set of eigenfunctions found by the method of separation of variables and evaluating these for level surfaces of the separable coordinate system [1], and b) evaluating the free space Green's function numerically at a set of points on a surface and using numerical matrix inversion techniques [2,3]. The first method has many advantages, including trouble-free numerical implementation, but has the fundamental limitation of being applicable only to level surfaces of separable coordinate systems. The second method is applicable to arbitrarily shaped surfaces, and does not require evaluating special functions (Bessel functions, spherical harmonics, etc.), but it has a substantial problem at certain frequencies (interior resonances of the shape) which is manifest as the ill-conditioning of the matrices for numerical inversion. A third, relatively new, method was introduced by Koopman [4] in 1989 and extended by Huang and Maynard [5,6]. This paper discusses some details of this method and presents some results from an application where the method was the only one which could correctly explain experimental measurements of radiation damping for objects of non-trivial shape vibrating in a high density gas [7]. Complete details and the source code for the computer programs have been available at the Web site ftp://ftp.phys.psu.edu/pub/maynard/sphwav, with a few updates, since their origin in 1996.

The key to the new method was the realization that solving the Surface Helmholtz Integral Equation numerically for an odd-shaped surface is not necessary if one fits data points with a set of functions which satisfy the Helmholtz equation. That is, functions which satisfy the Helmholtz equation automatically satisfy the Surface Helmholtz equation for any surface whatsoever. An actual physical surface will create a particular unique wave field which satisfies surface boundary conditions and the Surface Helmholtz Integral equation. However, once created, the wavefield may be expanded with a complete set of wavefunctions satisfying the Helmholtz equation, and each wave function will individually satisfy the Surface Helmholtz Integral equation, while the superposition of wavefunctions satisfies the particular boundary condition of the physical surface. This method seems similar to the original holography method, which also involved an expansion in eigenfunctions of the Helmholtz equation. However, in the new method, the expansion coefficients are not found with a theoretical decomposition on a level surface of a separable coordinate system, but instead are found by numerically fitting data (e.g. with a least-squares method) on whatever surface is convenient.

To implement this third method, data could be measured on an arbitrarily shaped surface, preferably one which closely surrounds the physical source. The measured data is then fit, with a least-squares numerical method, by adjusting the coefficients of a combination of solutions to the Helmholtz equation. For most sources, Spherical Wave Functions (SWF) would be a suitable choice for fitting data measured around the source. The same method works for the interior of source surfaces which radiate inward. By using Spherical Wave Functions for finite size sources, the problem of exponentially decaying evanescent fields is completely avoided.
In the section below, the method of solving boundary value problems for the Helmholtz equation with Spherical Wave Functions is discussed in some detail.

## 2 - EXPANSIONS WITH SPHERICAL WAVEFUNCTIONS

Assume a time dependence exp $(-i\omega t)$ and a complex sound pressure field $P(\vec{r}) = \mathrm{Re}\{P(\vec{r})\} + i\mathrm{Im}\{P(\vec{r})\}$ satisfying the Helmholtz equation with wavevector $k = \omega/c$. The complex particle velocity field is

$$\vec{v}(\vec{r}) = \frac{1}{ipck}\vec{\nabla}P(\vec{r}) \tag{1}$$

Using separation of variables, we find a complete set of complex linearly independent functions which radiate out to infinity (an important boundary condition). With three space variables, there must be two independent constants of separation and two mode labels. Thus we can write for these basis functions:

$$\nabla^2\Phi_{lm}(\vec{r}) + k^2\Phi_{lm}(\vec{r}) = 0 \tag{2}$$

Any solution to a radiation problem may be written as a linear combination of these functions:

$$P(\vec{r}) = \sum_l \sum_m A_{lm}\Phi_{lm}(\vec{r}) \tag{3}$$

Let $A_{lm} = a_{lm} + ib_{lm}$ and $\Phi_{lm}(\vec{r}) = R_{lm}(\vec{r}) + iS_{lm}(\vec{r})$, where the new constants and fields are purely real. Now

$$P(\vec{r}) = \sum_l \sum_m \left[\left(a_{lm}R_{lm}(\vec{r}) - b_{lm}S_{lm}(\vec{r})\right) + i\left(a_{lm}S_{lm}(\vec{r}) + b_{lm}R_{lm}(\vec{r})\right)\right] \tag{4}$$

The known boundary condition is the normal component of the particle velocity at a surface given by points $\vec{r}_s$. Note that the known surface velocity is purely real. We let the known data be given by the real function defined by

$$f(\vec{r}_s) = \rho c\hat{n}(\vec{r}_s)\cdot\vec{v}(\vec{r}_s) \tag{5}$$

where $\hat{n}(\vec{r}_s)$ is the unit normal at the surface point $\vec{r}_s$. Combining Eqs. 1, 4, and 5, we have

$$\begin{aligned} f(\vec{r}_s) &= \sum_l \sum_m \left[a_{lm}\left(\frac{1}{k}\hat{n}(\vec{r}_s)\cdot\vec{\nabla}S_{lm}(\vec{r}_s)\right) + b_{lm}\left(\frac{1}{k}\hat{n}(\vec{r}_s)\cdot\vec{\nabla}R_{lm}(\vec{r}_s)\right)\right] \\ &-i\sum_l \sum_m \left[a_{lm}\left(\frac{1}{k}\hat{n}(\vec{r}_s)\cdot\vec{\nabla}R_{lm}(\vec{r}_s)\right) - b_{lm}\left(\frac{1}{k}\hat{n}(\vec{r}_s)\cdot\vec{\nabla}S_{lm}(\vec{r}_s)\right)\right] \\ &= \sum_l \sum_m \left[\left(a_{lm}S'_{lm}(\vec{r}_s) + b_{lm}R'_{lm}(\vec{r}_s)\right) - i\left(a_{lm}R'_{lm}(\vec{r}_s) - b_{lm}S'_{lm}(\vec{r}_s)\right)\right] \end{aligned} \tag{6}$$

Since $f(\vec{r}_s)$ is purely real, the imaginary part of the left hand side of Eq. 6 must vanish. Now assume that the normal component of the particle velocity field is known at a finite set of discrete points $(\vec{r}_s)$ with $s = 1, 2, 3, ...N$. We simplify notation by writing $f(\vec{r}_s) = f_s$, and similarly for other functions of $\vec{r}_s$. We use the symbol $u$ as an index similar to $s$. We also simplify notation by letting the one integer $\mu$ index the two subscripts $l$ and $m$: $\mu = [l(\mu), m(\mu)]$. We truncate to a finite number of basis functions, so that $\mu = 1, 2, 3, ...L$. Let $\nu$ be an index similar to $\mu$. Finally, we use the convention that an index repeated in a term indicates a sum over that index. Now we can rewrite the real and imaginary parts of Eq. 6 as

$$f_s = S'_{s\mu}a_\mu + R'_{s\mu}b_\mu \tag{7}$$

$$R'_{s\mu}a_\mu = S'_{s\mu}b_\mu \tag{8}$$

Now $f_s$ is a vector of length $N$, $a_\mu$ and $b_\mu$ are vectors of length $L$, and $R'_{s\mu}$ and $S'_{s\mu}$ are $N$ and $L$ matrices. We shall have $N > L$, so that the matrices are not square. The method of Singular Value Decomposition (SVD) [8] allows one to find the inverse of such matrices. Let $T_{\nu\mu}$ be the inverse of $S'_{s\mu}$. Multiplying Eq. 8 by $T_{\nu\mu}$ solves for the vector $b$ in terms of the vector $a$ :

$$b_\nu = T_{\nu u} R'_{u\mu} a_\mu \tag{9}$$

Substituting Eq. 9 into Eq. 7 yields

$$f_s = \left(S'_{s\mu} + R'_{s\nu} T_{\nu u} R'_{u\mu}\right) a_\mu \tag{10}$$

Use SVD a second time to find the inverse of the matrix in parentheses in Eq. 10. Indicating this inverse with $Q_{\mu s}$ we now have $a_\mu = Q_{\mu s} f_s$. This is equivalent [8] to adjusting the coefficients $a_\mu$ to least-squares fit the boundary data $f_s$. With Eq. 9 we also have $b_\mu$, and from Eq. 4 we have $P\left(\vec{r}_s\right)$. With $P\left(\vec{r}_s\right)$ and $f\left(\vec{r}_s\right) = \rho c \hat{n}\left(\vec{r}_s\right) \cdot \vec{v}\left(\vec{r}_s\right)$, all other acoustic quantities may be calculated using closed-form expressions.
We separate variables in spherical coordinates $(r, \theta, \phi)$ but $\vec{r}_s$ and $\hat{n}\left(\vec{r}_s\right)$ will be given in cartesian coordinates (*x, y, z*). We make all lengths non-dimensional by multiplying by the wavenumber $k = \omega/c$. We simplify notation by letting $kx \rightarrow x, ky \rightarrow y, kz \rightarrow z, kr \rightarrow r$, and $(1/k)\,\vec{\nabla} \rightarrow \vec{\nabla}$. We also define $\zeta = \cos\theta$.
Separating variables in spherical coordinates yields the spherical wave functions:

$$\Phi_{lm}(r, \theta, \phi) = \left(j_l(r) + i y_l(r)\right)\left(\cos m\phi + \sin m\phi\right) Y_{lm}(\cos\theta) \tag{11}$$

where $Y_{lm}(\zeta) = \sqrt{\left((2l+1)/4\pi\right)\left((l-m)!/(l+m)!\right)} P_l^m(\zeta)$. The $j_l$ and $y_l$ are the spherical Bessel functions, and the $P_l^m$ are the associated Legendre polynomials. The $Y_{lm}$ are similar to the spherical harmonics, but with the $\phi$ dependence removed; the $\phi$ dependence is included explicitly in Eq. 11. Note that $-l \le m \le l$. The expression for $Y_{lm}$ is for $m \ge 0$ only; for $m < 0$ we use the Condon and Shortley phase: $Y_{l,-m}(\zeta) = (-1)^m Y_{lm}(\zeta)$. We truncate the number of basis functions by letting $L_{\max}$ be the highest order for the spherical Bessel functions. The total number of basis functions is $(L_{\max}+1)^2$. The real and imaginary parts of $\Phi_{lm}$ and their derivatives are readily determined. A Jacobian relates quantities in the spherical coordinate system to the data in cartesian coordinates. Details are available in an earlier paper [9].
It should be noted that some functions may have indeterminate forms (e.g. when $\cos\theta = \pm 1$), but these may be handled analytically [9]. The spherical Bessel functions and the associated Legendre functions may be calculated by computer using the upward and downward recursion relations [8]. The derivatives of the functions may also be found by computer using standard relations with lower order functions.

## 3 - TESTING AND APPLYING THE SWF METHOD TO ACTUAL MEASUREMENTS

The SWF computer programs were developed in response to a request to explain some experimental measurements on elastic solids vibrating in a high pressure (high density) gas. When the solids were driven at resonance frequencies, the quality factors (Q's) were lowered as a result of the radiation of sound energy into the surrounding gas. While the solids had simple shapes (rectangular parallelepipeds) they were not level surfaces of a separable coordinate system, and the usual approximations (e.g. each face radiating independently as a baffled planar source) did not agree with the experimental data. The SWF calculation gave very good agreement.
In order to test the computer programs, some model sources were devised. One set of sources were spheres with vibrating end-caps; the computer programs gave correct results for both real and imaginary parts, as found in Morse [10]. Other model test sources had non-trivial shapes (cubes), but with surface velocities which yielded theoretically predictable power radiation at very low and very high frequencies. Two of these cube sources, as well as two of the modes of the resonating elastic solids discussed above, are illustrated in Fig. 1.
One cube source had four rigid side faces, and the top and bottom faces oscillated in phase (outwardly), as indicated by the arrows in Fig. 1a. At very low frequencies this would radiate as a simple monopole source. Another cube source had the top and bottom faces oscillating out of phase, as indicated by the arrows in Fig. 1b. At very low frequencies this would radiate as a simple dipole source. At high frequencies, the vibrating surfaces of the two model test sources would be highly directional, and could be treated as independent baffled planar sources. Figs. 1c and 1d illustrate two of the normal modes of vibration of the elastic solid which was measured experimentally. It should be noted that the SWF method does the equivalent of determining the multipole strengths of these sources in the difficult frequency range where the size of the source is near the wavelength in the sound medium.

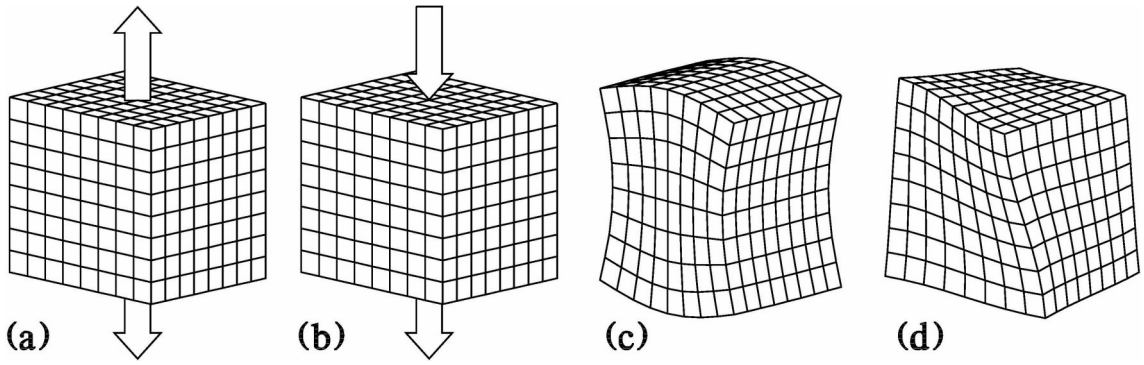


**Figure 1:** Model test sources and experimentally measured sources; (a) model source with faces oscillating in phase, a simple monopole at low frequencies; (b) model source with faces oscillating out of phase, a simple dipole at low frequencies; (c) and (d) modes of vibration of an elastic solid whose sound power radiation was measured experimentally.

The results of the SWF calculations are presented in Fig. 2. Each section shows the power radiated versus frequency, expressed as the sample size (the edge length of the cube, $E$) divided by the sound wavelength $\lambda$. Figs. 2a through 2d are for the sources presented in Figs. 1a through 1d, respectively. In Figs. 1a and 1b, the bold lines at the lower left and upper right indicate the theoretical limits for very low and very high frequencies. The SWF calculated results are square points and the lines through them are simply a guide to the eye. For Fig. 2a, the power varies as $(E/\lambda)^2$ at low frequencies, as for a monopole source. For Fig. 2b, the power varies as $(E/\lambda)^4$ at low frequencies, as for a dipole source. For both Fig. 2a and 2b, the variation in the data at high frequency is not scatter, but is an oscillation of the power for frequencies where $E/\lambda \approx 1$.

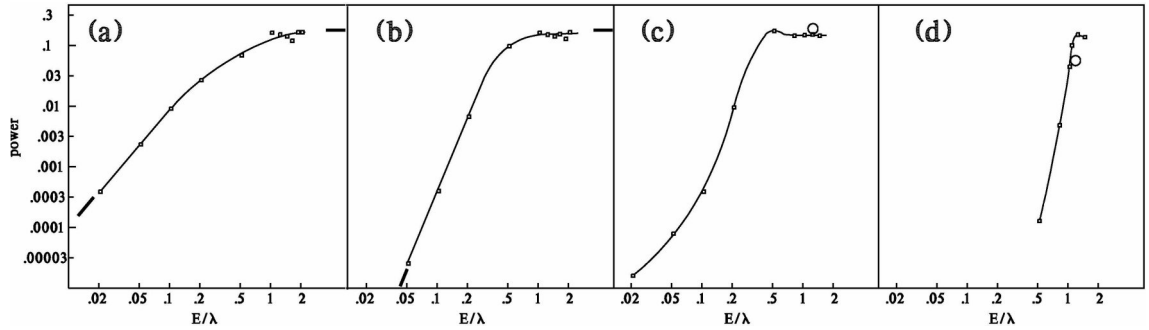


**Figure 2:** Results of the spherical wave function calculations; figures (a) through (d) are for the sources indicated in Fig. 1a through 1d respectively.

Figs. 2c and 2d show the interesting frequency dependence of the surface velocity fields indicated in Figs. 1c and 1d. Of course, in the experimental measurements the solid was oscillating a just one natural frequency. The experimental results at the appropriate frequencies are indicated by the open circles in Figs. 2c and 2d. Although the experimental accuracy was limited, the results are in agreement at a 15 % level. Calculations with methods other than the SWF method gave results which were in error by a factor of 3.

**ACKNOWLEDGEMENTS**
This research was supported by the Office of Naval Research.

**REFERENCES**

1. **J. D. Maynard, E. G. Williams, and Y. Lee**, Nearfield Acoustic Holography: I. Theory of generalized holography and the development of NAH, *J. Acoust. Soc. Am.*, Vol. 78, pp. 1395-1413, 1985

2. **W. A. Veronesi and J. D. Maynard**, Nearfield Acoustic Holography (NAH II. Holographic reconstruction algorithms and computer implementation, *J. Acoust. Soc. Am.*, Vol. 81, pp. 1307-1322, 1987

3. **W. A. Veronesi and J. D. Maynard**, Digital holographic reconstruction of sources with arbitrarily shaped surfaces, *J. Acoust. Soc. Am*, Vol. 85, pp. 588-598, 1989

4. **G. H. Koopman, L. Song, and J. B. Fahnline**, A method for calculating acoustic fields based on the principle of wave superposition, *J. Acoust. Soc. Am.*, Vol. 86, pp. 2433-2438, 1989

5. **Y. Huang**, *Computer techniques for three-dimensional source radiation*, The Pennsylvania State University, 1990

6. **J. D. Maynard**, Nearfield acoustic holography and arbitrarily shaped sources, In *International Meeting on Acoustical Imaging*, pp. 25-30, 1994

7. **L. E. Hargrove and J. D. Maynard**, Determining the radiation impedance of arbitrarily shaped vibrating surfaces, In *Private communication and Resonance Meeting*, 1996

8. **W. H. Press, S. A. Teukolsky, W. T. Vettering, and B. P. Flannery**, *Numerical Recipes*, Cambridge University Press, 1992

9. **J. D. Maynard**, Nearfield acoustic holography and arbitrarily shaped sources and enclosures, In *Sixth International Conference on Sound and Vibration*, 1999

10. **P. M. Morse**, *Vibration and Sound*, McGraw-Hill, pp. 325, 1948